

# Viscous and resistive eddies near a sharp corner

By H. K. MOFFATT

Trinity College, Cambridge

(Received 20 June 1963)

Some simple similarity solutions are presented for the flow of a viscous fluid near a sharp corner between two planes on which a variety of boundary conditions may be imposed. The general flow near a corner between plane boundaries at rest is then considered, and it is shown that when either or both of the boundaries is a rigid wall and when the angle between the planes is less than a certain critical angle, any flow sufficiently near the corner must consist of a sequence of eddies of decreasing size and rapidly decreasing intensity. The ratios of dimensions and intensities of successive eddies are determined for the full range of angles for which the eddies exist. The limiting case of zero angle corresponds to the flow at some distance from a two-dimensional disturbance in a fluid between parallel boundaries. The general flow near a corner between two plane free surfaces is also determined; eddies do not appear in this case. The asymptotic flow at a large distance from a corner due to an arbitrary disturbance near the corner is mathematically similar to the above, and has comparable properties. When the fluid is electrically conducting, similarity solutions may be obtained when the only applied magnetic field is that due to a line current along the intersection of the two planes; it is shown that the effect of such a current is to widen the range of corner angles for which eddies must appear.

## 1. Introduction

It is well known that the Stokes equation for the stream function  $\psi(r, \theta)$ ,  $\nabla^4\psi = 0$ , admits separated solutions in plane polar co-ordinates  $(r, \theta)$  of the form

$$\psi = r^\lambda f_\lambda(\theta), \quad (1.1)$$

where  $\lambda$  is any number, real or complex, which may conveniently be called the *exponent* of the corresponding solution. In general the form of the function  $f_\lambda(\theta)$ , involving four arbitrary constants,  $A$ ,  $B$ ,  $C$  and  $D$ , is

$$f_\lambda(\theta) = A \cos \lambda\theta + B \sin \lambda\theta + C \cos(\lambda - 2)\theta + D \sin(\lambda - 2)\theta; \quad (1.2)$$

in the particular cases when  $\lambda = 0, 1$  or  $2$ , this solution degenerates to the forms

$$f_0(\theta) = A + B\theta + C\theta^2 + D\theta^3, \quad (1.3)$$

$$f_1(\theta) = A \cos \theta + B \sin \theta + C\theta \cos \theta + D\theta \sin \theta, \quad (1.4)$$

$$f_2(\theta) = A \cos 2\theta + B \sin 2\theta + C\theta + D. \quad (1.5)$$

These solutions are relevant to the flow between two plane boundaries meeting at a sharp corner. The boundaries may be rigid walls on which the fluid velocity is prescribed, or surfaces on which the stress is prescribed (the pressure distribu-

tion on the surface being such as to keep it plane). Three distinct categories of flow can be described by these separated solutions. In the first category, a non-zero velocity or stress is prescribed on one or both boundaries, and the flow is described by a particular integral of the biharmonic equation satisfying appropriate *inhomogeneous* boundary conditions. One such situation has been described by Taylor (1960); this arises when one rigid plane is scraped along another at a constant velocity and angle. This and related situations are considered in §2; in each of these situations, the exponent  $\lambda$  is a positive integer, whose value is determined on dimensional grounds.

In the second category either the velocity or the tangential stress vanishes on each boundary. The flow near the corner is induced by a general motion at a large distance from the corner; for example, fluid may be driven into the corner near one of the boundaries and out of the corner near the other—such a flow might be realized near the corners of a triangular container of viscous fluid when a cylinder is rotated anywhere inside it. In this case, the complementary function of the biharmonic equation is sought, satisfying *homogeneous* boundary conditions. This problem seems to have been first considered by Rayleigh (1920), who showed that no solution of the form (1.1) with integral exponent could satisfy the four boundary conditions. Later Dean & Montagnon (1948) showed that for angles between the planes less than about  $146^\circ$ , the exponent is necessarily complex. In this paper, this result is interpreted as implying the existence of an infinite sequence of eddies near the corner; the structure of these eddies is described in §3. It is interesting that viscosity, usually a damping mechanism, is here responsible for the *generation* of a geometrical progression of eddies. The damping mechanism, however, is still present, and the ratio of the intensities of successive eddies is high. Even in the most favourable circumstance it is greater than 300, so that, although it should be easy enough to observe one such eddy, to observe a sequence of eddies might present insurmountable experimental difficulties. The presence of at least one solid boundary is essential to the formation of eddies; the flow between two free surfaces† is determined in §3, and the appropriate exponent is always real.

The flows in this second category all have finite velocity at the corner  $r = 0$ . This implies that the real part of the exponent  $\lambda$  is greater than unity. If the real part of  $\lambda$  is less than unity, the velocity in the corresponding flow is infinite at  $r = 0$  but tends to zero as  $r \rightarrow \infty$ . Such solutions may describe the flow at a large distance from the intersection of two planes when some steady disturbance is present near the origin. This is the third category of possible flows, and is considered in §4. Eddies appear also in this case; the dimensions of successive eddies increase with distance from the corner and their intensities decrease in the same ratios (for a given angle) as for the flows of the second category.

In all cases, it is important to determine for what range of values of  $r$  the Stokes approximation is valid. If (for the moment) we write (1.1) in the form

$$\psi = Ar^\lambda f(\theta)$$

† In this paper, the term ‘free surface’ is used to describe a fluid surface that is not bounded by a rigid wall; it may, however, be subjected to tangential and normal stresses.

where  $A$  is a dimensional constant and  $f(\theta)$  is of order unity, then the corresponding velocity  $\mathbf{u}$  is of order  $Ar^p$  where  $p$  is the real part of  $\lambda - 1$ . The orders of magnitude of the inertial acceleration  $\mathbf{u} \cdot \nabla \mathbf{u}$  and the viscous force  $\nu \nabla^2 \mathbf{u}$  are then given by  $\mathbf{u} \cdot \nabla \mathbf{u} = O(A^2 r^{2p-1})$ ,  $\nu \nabla^2 \mathbf{u} = O(\nu A r^{p-2})$ , so that the inertial term is negligible provided

$$R = \frac{Ar^{p+1}}{\nu} \ll 1,$$

where  $R$  is the Reynolds number based on distance from the corner. Hence if  $\text{Re}(\lambda) > 0$ , inertia forces are negligible for sufficiently *small*  $r$ , while if  $\text{Re}(\lambda) < 0$ , inertia forces are negligible for sufficiently *large*  $r$ . In the critical case in which  $\lambda = 0$ ,  $A$  has the same dimensions as  $\nu$ , and the Reynolds number is independent of  $r$ . The corresponding solution, in which velocities are proportional to  $r^{-1}$ , is simply the low Reynolds number limit of the exact solution of the Navier-Stokes equations representing the flow due to a source or sink at the intersection of two plane boundaries (Jeffery 1915).

It is interesting to inquire whether magnetohydrodynamic forces can significantly alter the effects outlined above. Similarity solutions of the type (1.1) still exist when the only applied magnetic field is that due to a line current along the intersection of the two planes. Physical intuition suggests that increasing the current will provide a Lorentz force in the fluid which tends to promote the formation of eddies near the corner. It is shown in §5 that when a Hartmann number based on the line current strength is equal to unity, eddies form, no matter what the angle between the bounding planes. Even if this angle is reflex, the same effect occurs, so that, for example, the Stokes flow near the leading edge of a wedge has the character of an infinite sequence of eddies if a sufficiently strong line current flows along the leading edge; the edge is in a sense shielded from the external flow.

## 2. Some simple similarity solutions when a velocity or stress is prescribed

The particular situation considered by Taylor (1960) is sketched in figure 1(a). The plane  $\theta = \alpha$  is at rest and the plane  $\theta = 0$  is scraped along parallel to itself with velocity  $U$ . Near the corner, where the Stokes approximation is valid, the stream function is independent of kinematic viscosity  $\nu$ , and dimensional analysis shows that  $\psi$  must be of the form  $\psi = Ur f_1(\theta)$ ; the corresponding velocity components are

$$u = \frac{1}{r} \frac{\partial \psi}{\partial \theta} = U f_1'(\theta), \quad v = -\frac{\partial \psi}{\partial r} = -U f_1(\theta).$$

The boundary conditions

$$f_1(0) = 0, \quad f_1'(0) = 1, \quad f_1(\alpha) = f_1'(\alpha) = 0,$$

determine the constants  $A$ ,  $B$ ,  $C$  and  $D$  in (1.4), giving after a little simplification

$$f_1 = -(\sin^2 \alpha - \alpha^2)^{-1} \{ \alpha(\theta \sin \theta - \alpha \sin \alpha) - \theta \sin(\theta - \alpha) \sin \alpha \}. \quad (2.1)$$

A similar situation arises when a flat plate is drawn into a viscous fluid with a free surface (figure 1(b)). Surface tension is neglected, and it is supposed that

gravity keeps the free surface horizontal. The boundary conditions for the situation of figure 1*b* are

$$f_1(-\alpha) = 0, \quad f_1'(-\alpha) = 1, \quad f_1(0) = f_1'(0) = 0,$$

and the corresponding form of  $f_1(\theta)$  is

$$f_1(\theta) = (\sin \alpha \cos \alpha - \alpha)^{-1} (\theta \cos \theta \sin \alpha - \alpha \cos \alpha \sin \theta). \quad (2.2)$$

The velocity of particles on the free surface is

$$u_s = U f_1'(0) = -U \left( \frac{\sin \alpha - \alpha \cos \alpha}{\alpha - \sin \alpha \cos \alpha} \right) = -U \left\{ 1 - \frac{(\alpha - \sin \alpha)(1 + \cos \alpha)}{\alpha - \sin \alpha \cos \alpha} \right\}. \quad (2.3)$$

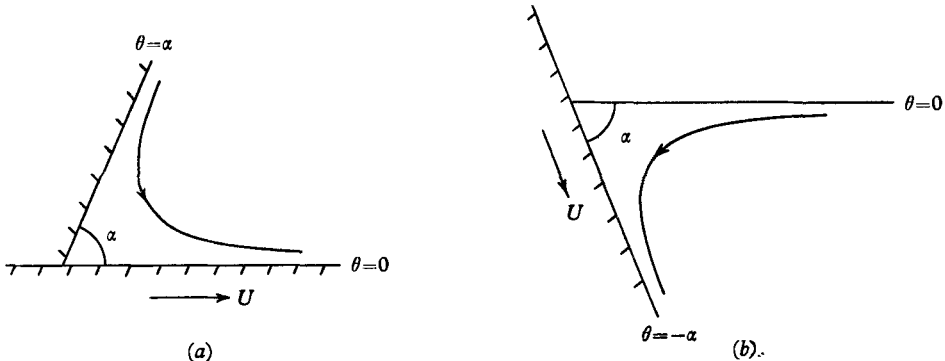


FIGURE 1. Flow in a corner, characterized by a boundary velocity  $U$ .

The second form for  $u_s$  shows that the fluid particles on the free surface move towards the corner with a speed independent of  $r$  and less than the speed of the plate  $U$ . The speed of the particles suddenly increases to the value  $U$  as they meet the plate and turn the corner. This infinite acceleration is brought about by an infinite stress and pressure (both of order  $r^{-1}$ ) on the plate at the corner. The solution breaks down very near the corner where the free surface must be distorted both by surface tension and by pressure gradients of the order of the weight (per unit volume) of the fluid.

Certain simple flows exist that are described in a similar way by stream functions of the type (1.1) with exponent  $\lambda = 2$ . Consider, for example, the flow between two hinged planes  $\theta = \pm \alpha$  which rotate relative to each other with angular velocity  $-2\omega$  (figure 2*a*). The bisecting plane may be chosen as the plane  $\theta = 0$ . The flow is unsteady ( $d\alpha/dt = -\omega$ ), but the acceleration terms of the equations of motion are negligible in the region near 0 defined by  $\omega r^2/\nu \ll 1$ . The stream function must, on dimensional grounds, be of the form

$$\psi = \omega r^2 f_2(\theta). \quad (2.4)$$

The boundary conditions implied in figure 2*a* are

$$f_2(\alpha) = -f_2(-\alpha) = \frac{1}{2}, \quad f_2'(\alpha) = f_2'(-\alpha) = 0.$$

Applying these to the function (1.5) gives the appropriate solution

$$f_2(\theta) = \frac{1}{2} (\sin 2\alpha - 2\alpha \cos 2\alpha)^{-1} (\sin 2\theta - 2\theta \cos 2\alpha). \quad (2.5)$$

The streamlines are indicated in the figure. The corresponding pressure distribution is of order  $\log r$  near the corner. The same solution, in the region  $-\alpha \leq \theta \leq 0$  alone, describes the flow between a rotating plane and a horizontal free surface. (Here again, surface tension and large pressure gradients must distort the free surface very near the corner.)

Another example of a flow that is described by a solution with exponent  $\lambda = 2$  is sketched in figure 2 (b). Here the wall  $\theta = 0$  is at rest and a constant stress  $\tau$  is applied to the free surface  $\theta = \alpha$ . The boundary conditions are

$$u = v = 0 \quad \text{on} \quad \theta = 0; \quad v = 0, \quad \frac{1}{r} \frac{\partial v}{\partial \theta} = \frac{\tau}{\nu \rho} \quad \text{on} \quad \theta = \alpha.$$

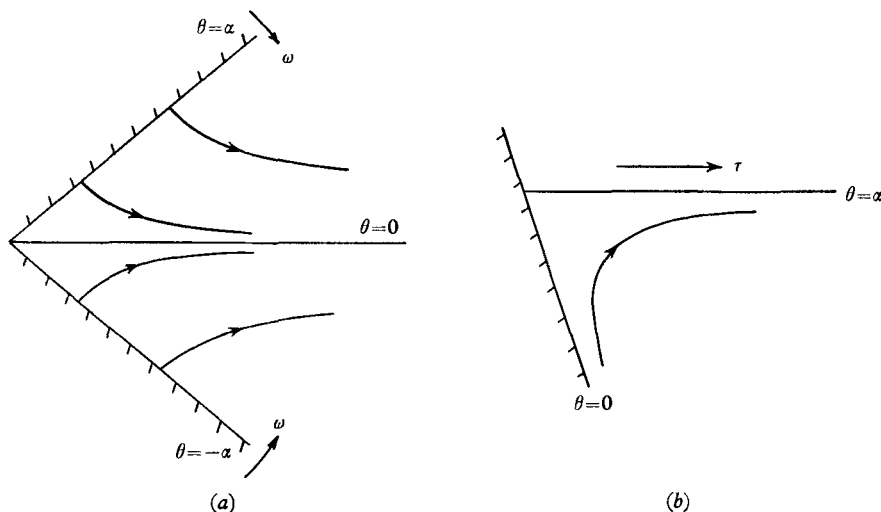


FIGURE 2. Flow in a corner characterized (a) by an angular velocity  $\omega$ , and (b) by a surface stress  $\tau$ .

Hence  $\psi$  is proportional to  $\tau/\nu\rho$  and must take the form

$$\psi = \frac{\tau}{\nu\rho} r^2 f_2(\theta)$$

with boundary conditions

$$f_2(0) = f_2'(0) = 0, \quad f_2'(\alpha) = 0, \quad f_2''(\alpha) = \frac{1}{2}.$$

These define the solution

$$f_2(\theta) = \frac{1}{8}(\cos 2\alpha - 1)^{-1} \{(\cos 2\alpha - 1) \cos 2\theta + \sin 2\alpha \sin 2\theta - 2\theta \sin 2\alpha + 1\}. \quad (2.6)$$

### 3. Flow near a sharp corner induced by an arbitrary disturbance at a large distance

If two rigid boundaries are fixed at an angle  $2\alpha$ , it is possible to induce a flow near the corner simply by stirring the distant fluid. It may be anticipated that the flow pattern sufficiently near the corner may be to some extent independent of the nature of the energy input at a large distance. It is the purpose of this section to describe the nature of the asymptotic flow near the corner. A mathematical

solution of this problem was partially determined by Dean & Montagnon (1948), but the solution will be rederived here in a form more amenable to interpretation.

We assume that in the Stokes régime the stream function can be expanded in a series† of the form

$$\psi = \sum_1^{\infty} A_n r^{\lambda_n} f_{\lambda_n}(\theta), \quad (3.1)$$

where the  $\lambda_n$  are suitably chosen and ordered so that

$$1 < \text{Re}(\lambda_1) < \text{Re}(\lambda_2) < \dots$$

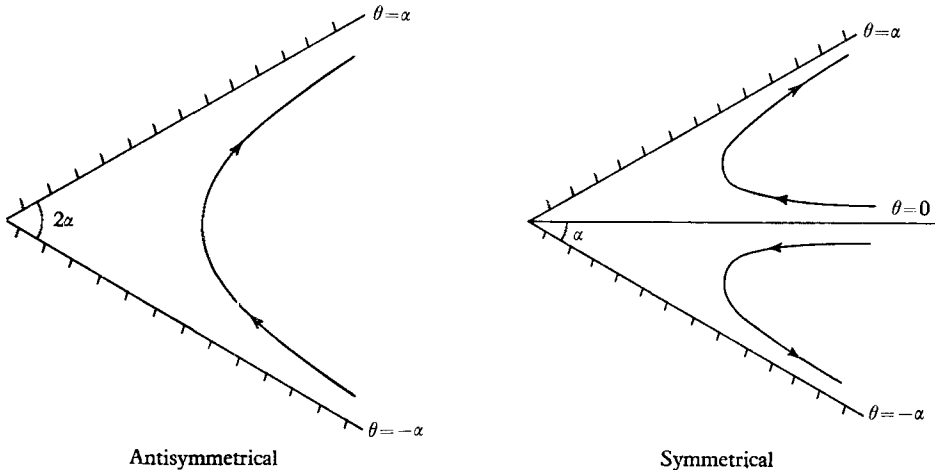


FIGURE 3. Flow in a corner between rigid boundaries, induced by an arbitrary two-dimensional agitation at a large distance.

The  $A_n$  are constants. If the  $\lambda_n$  are complex, the real part of (3.1) is understood to be relevant. The first of the inequalities following (3.1) ensures that the velocity vanishes at the intersection. Sufficiently near the corner the first term dominates and

$$\psi \sim A_1 r^{\lambda_1} f_{\lambda_1}(\theta), \quad (3.2)$$

provided  $A_1 \neq 0$ .

Clearly the stirring force may produce either an anti-symmetrical or a symmetrical flow pattern near the corner (figure 3). The corresponding stream function  $\psi(r, \theta)$  is an even or odd function of  $\theta$ , respectively. The general flow will of course be a mixture of the two, but it is convenient (and permissible, in view of the linearity of the Stokes equation) to consider the types separately. In the symmetrical flow, the stress component  $(1/r)\partial u/\partial\theta$  vanishes on  $\theta = 0$ , so that again the flow between a rigid boundary and a free surface ( $\theta = 0$ ) will be

† One particular case, in which the outer stirring mechanism is specified, has been completely solved and the constants  $A_n$  in the expansion (3.1) obtained explicitly. It is supposed that the motion is generated by the motion of 'sleeves' inserted in the boundaries  $\theta = \pm\alpha$  in the region  $a \leq r \leq b$ , each sleeve moving with uniform velocity  $V$ . The problem is solved using the Mellin transform, and the series (3.1) emerges as the sum of the residues at poles in a contour integral. The details of this solution are in course of publication (Moffatt 1964).

simultaneously determined. If  $2\alpha > \pi$ , the flow is that round or past the leading edge of a wedge (figure 4).

The spreading of the streamlines implied by the retardation as the corner is approached is worth noticing. The streamline pattern in the antisymmetric case is to be contrasted with that of the potential flow of an inviscid fluid.

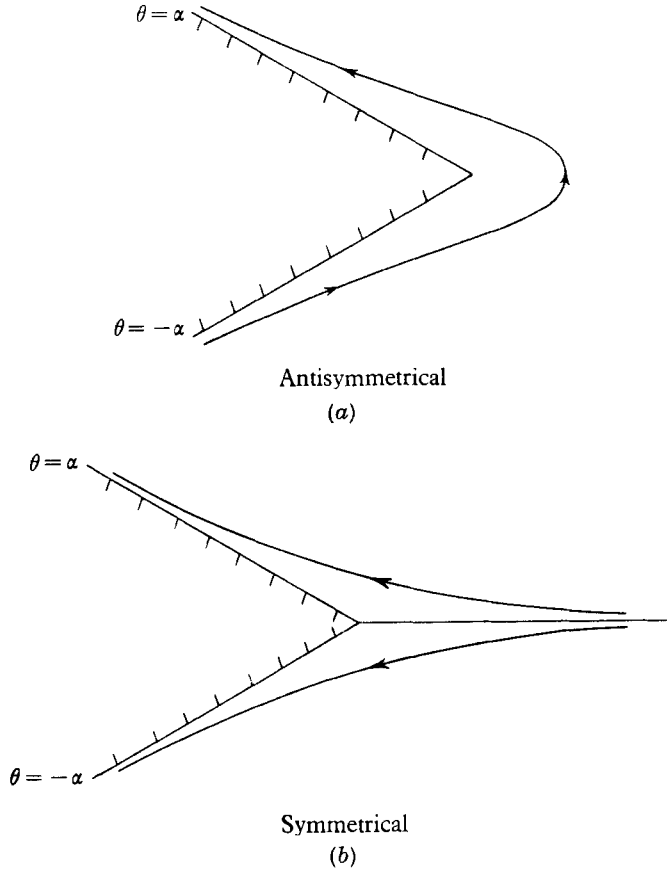


FIGURE 4. The general viscous flow near a corner of reflex angle.

3.1. *Antisymmetric flow between rigid boundaries*

For this type of flow,  $f_\lambda(\theta)$  is even, so that the constants  $B$  and  $D$  in (1.2) vanish and

$$f_\lambda(\theta) = A \cos \lambda\theta + C \cos (\lambda - 2)\theta. \tag{3.3}$$

Both velocity components vanish on  $\theta = \pm \alpha$  provided  $f(\pm \alpha) = f'(\pm \alpha) = 0$ , so that

$$\left. \begin{aligned} A \cos \lambda\alpha + C \cos (\lambda - 2)\alpha &= 0, \\ A \lambda \sin \lambda\alpha + C(\lambda - 2) \sin (\lambda - 2)\alpha &= 0, \end{aligned} \right\} \tag{3.4}$$

Hence for a non-trivial solution,  $\lambda$  satisfies an equation which reduces to the form

$$\sin 2\mu\alpha = -\mu \sin 2\alpha \quad \text{where} \quad \mu = \lambda - 1. \tag{3.5}$$

It was noticed by Dean & Montagnon that when  $2\alpha$  is less than a critical angle  $2\alpha_1$  say, approximately equal to  $146^\circ$ , this equation admits no real solutions (other than  $\mu = 0$  which is physically irrelevant here, since for  $\lambda = 1$  the appropriate form for  $f_\lambda(\theta)$  is (1.4) rather than the form (3.3) used above). As  $2\alpha$  increases from  $2\alpha_1$  to  $\pi$ , the number of real solutions of (3.5) increases from one to infinity.

The complex solutions, when  $2\alpha < 2\alpha_1$ , may be determined by writing  $\mu = p + iq$ , whereupon (3.5) gives the two real equations

$$\begin{aligned}\sin 2\alpha p \cosh 2\alpha q &= -p \sin 2\alpha, \\ \cos 2\alpha p \sinh 2\alpha q &= -q \sin 2\alpha,\end{aligned}$$

or, in terms of the variables  $\xi = 2\alpha p$ ,  $\eta = 2\alpha q$  and the positive parameter  $k = \sin 2\alpha/2\alpha$ ,

$$\left. \begin{aligned}\sin \xi \cosh \eta &= -k\xi, \\ \cos \xi \sinh \eta &= -k\eta.\end{aligned} \right\} \quad (3.6)$$

$2\alpha^\circ$	$\xi_1$	$\eta_1$	$\ln \rho_1$	$\ln \varpi_1$	$\xi_2$	$\eta_2$	$\ln \rho_2$	$\ln \varpi_2$
0	4.21	2.26	0.00	5.87	7.50	2.76	0.00	8.53
10	4.21	2.25	0.24	5.87	7.50	2.76	0.198	8.53
30	4.22	2.20	0.75	6.02	7.50	2.72	0.606	8.66
50	4.24	2.11	1.30	6.32	7.52	2.63	1.04	9.07
70	4.26	1.97	1.94	6.79	7.54	2.51	1.53	9.64
90	4.30	1.77	2.79	7.63	7.57	2.32	2.13	10.43
110	4.35	1.47	4.10	9.29	7.61	2.02	3.00	11.83
130	4.42	1.02	6.98	13.60	7.66	1.62	4.40	14.85
140	4.46	0.64	11.91	21.75	7.68	1.35	5.68	17.89
$2\alpha_1$	4.48	0.00	$\infty$	$\infty$	—	—	—	—
150	—	—	—	—	7.70	0.95	8.65	25.20
$2\alpha_2$	—	—	—	—	7.73	0.00	$\infty$	$\infty$

TABLE 1. Length and velocity scale factors for corner eddies.

Clearly, any solution  $(\xi_n, \eta_n)$  of these equations must be such that both  $\sin \xi_n$  and  $\cos \xi_n$  are negative, and this condition is satisfied provided

$$(2n-1)\pi < \xi_n < (2n-\frac{1}{2})\pi. \quad (3.7)$$

It is, moreover, not difficult to see that there is a solution  $(\xi_n, \eta_n)$  of (3.6) with  $\xi_n$  in the range (3.7). The corresponding eigenvalue  $\lambda_n$  is given by

$$\lambda_n = 1 + (2\alpha)^{-1}(\xi_n + i\eta_n). \quad (3.8)$$

Interest centres chiefly on the value of  $\lambda_1$ , since as observed already (equation (3.2)), it will determine the asymptotic behaviour near the corner. The values of this quantity corresponding to angles  $2\alpha$  greater than  $\frac{1}{2}\pi$  were given by Dean & Montagnon. We are more interested here in acute angles, and the values of  $\xi_1$  and  $\eta_1$  as calculated from (3.6) for different values of the angle  $2\alpha$  are given in table 1. The corresponding values of  $\lambda_1$  may be easily deduced.

The interesting feature of the solution that is implied by the complex exponent is the sequence of eddies that must be induced near the origin. To see this it is simply necessary to write the asymptotic stream function in the form

$$\begin{aligned}\psi &\sim r^{\lambda_1}(A \cos \lambda_1 \theta + C \cos (\lambda_1 - 2)\theta) \\ &= A' \left(\frac{r}{r_0}\right)^{\lambda_1} [\cos \lambda_1 \theta \cos (\lambda_1 - 2)\alpha - \cos (\lambda_1 - 2)\theta \cos \lambda_1 \alpha],\end{aligned} \quad (3.9)$$



where  $A' = Ar_0^{\lambda_1} \sec(\lambda_1 - 2)\alpha$ ,  $r_0$  being an arbitrary length scale, whose significance will emerge later. The transverse component of velocity on the plane  $\theta = 0$  is then

$$v_{\theta=0} = - \left( \frac{\partial \psi}{\partial r} \right)_{\theta=0} \sim (a + ib) \frac{1}{r} \left( \frac{r}{r_0} \right)^{\lambda_1},$$

where  $a + ib = -\lambda_1 A' [\cos(\lambda_1 - 2)\alpha - \cos \lambda_1 \alpha]$ .

Now

$$\begin{aligned} \left( \frac{r}{r_0} \right)^{\lambda_1} &= \left( \frac{r}{r_0} \right)^{p_1+1+iq_1} = \left( \frac{r}{r_0} \right)^{p_1+1} \exp(iq_1 \ln r/r_0) \\ &= \left( \frac{r}{r_0} \right)^{p_1+1} \left[ \cos \left( q_1 \ln \frac{r}{r_0} \right) + i \sin \left( q_1 \ln \frac{r}{r_0} \right) \right], \end{aligned}$$

and since the real part of the expression for  $v_{\theta=0}$  is understood, we have

$$\begin{aligned} v_{\theta=0} &\sim \operatorname{Re}(a + ib) \frac{1}{r} \left( \frac{r}{r_0} \right)^{p_1+1} \left[ \cos \left( q_1 \ln \frac{r}{r_0} \right) + i \sin \left( q_1 \ln \frac{r}{r_0} \right) \right] \\ &= \gamma \frac{1}{r} \left( \frac{r}{r_0} \right)^{p_1+1} \sin \left( q_1 \ln \frac{r}{r_0} + \epsilon \right), \text{ say.} \end{aligned} \quad (3.10)$$

This expression changes sign infinitely often as the point  $r = 0$  is approached. In fact  $v_{\theta=0} = 0$  for values of  $r$  satisfying

$$q_1 \ln \frac{r}{r_0} + \epsilon = -n\pi \quad (n = 0, 1, 2, \dots),$$

i.e.  $r = r_0 (e^{-\epsilon/q_1}) e^{-n\pi/q_1} = r_n$ , say. (3.11)

It is clear that  $r_n$  is the distance of the centre of the  $n$ th eddy (counted from any chosen eddy) from the corner. Note that

$$\frac{r_n}{r_{n+1}} = \frac{r_n - r_{n+1}}{r_{n+1} - r_{n+2}} = e^{\pi/q_1}, \quad (3.11a)$$

so that the dimensions of successive eddies fall off in geometric progression with common ratio  $\rho_1 = e^{\pi/q_1}$ , depending only on the angle  $2\alpha$  as the corner is approached. The absolute size of the eddies, however, is proportional to the length scale  $r_0$ , which is determined (as is the parameter  $\epsilon$ ) by conditions far from the corner where the stirring forces agitate the fluid.

The velocity  $v_{\theta=0}$  has a local maximum at the points

$$r = r_{n+\frac{1}{2}} = (r_0 e^{-\epsilon/q_1}) \exp \left[ - (n + \frac{1}{2}) \pi / q_1 \right],$$

and the velocity at these points is

$$v = \frac{\gamma}{r_0^{p_1+1}} r_{n+\frac{1}{2}}^{p_1+1} = v_{n+\frac{1}{2}}, \text{ say.}$$

This may be taken as a measure of the 'intensity' of consecutive eddies. The intensities therefore fall off in geometric progression with common ratio

$$\omega_1 = \frac{v_{n+\frac{1}{2}}}{v_{n+\frac{3}{2}}} = \left( \frac{r_{n+\frac{1}{2}}}{r_{n+\frac{3}{2}}} \right)^{p_1} = e^{\pi p_1 / q_1}, \quad (3.12)$$

a quantity which also depends only on the angle  $2\alpha$ .

The parameters  $\rho_1$  and  $\varpi_1$  seem to provide the best description of this sequence of eddies; their logarithms are given in table 1, and these are displayed for the relevant range of the angle  $2\alpha$  in figure 5. It will be observed that  $\rho_1$  is of order unity, so that adjacent eddies are of comparable size, for values of  $2\alpha$  up to about  $40^\circ$ , but for larger corner angles  $\rho_1$  increases to about 10 at  $2\alpha = 90^\circ$  and very

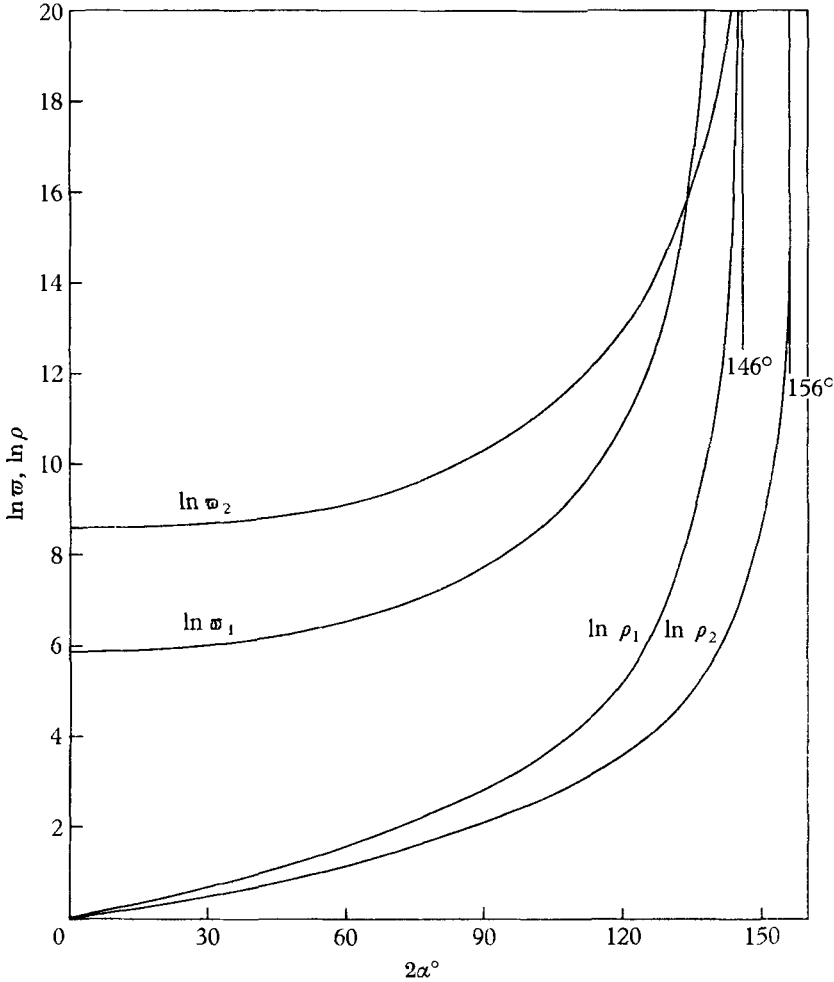


FIGURE 5. Intensity and scale factors for symmetric and antisymmetric corner eddies.

rapidly when  $2\alpha$  approaches  $146^\circ$ . The relative intensity of adjacent eddies is always large, its minimum value,  $\varpi_{\min} \approx 365$ , being attained in the limiting case  $2\alpha = 0$ . For a right angle,  $\varpi_1 \approx 2000$  and the eddy intensity falls off very rapidly as the corner is approached. The relative eddy sizes and intensities are indicated in figure 6 for two different corner angles,  $2\alpha = 20^\circ$  and  $60^\circ$ . The relative dimensions of the eddies are approximately correct, but their shapes have not been calculated exactly and are only indicated schematically. All the eddies (for a given corner angle) are geometrically and dynamically similar, but with successive changes of length and velocity scales represented by the factors  $\rho_1$  and  $\varpi_1$ .

When  $2\alpha > 146^\circ$ , equation (3.5) has a real solution  $\mu$  which was tabulated by Dean & Montagnon. It decreases continuously from the value 1.76 when  $2\alpha = 146^\circ$  through 1.00 when  $2\alpha = 180^\circ$  (simple shear flow) to 0.50 when  $2\alpha = 360^\circ$  (flow round the edge of a flat plate). Thus eddies do not appear under general conditions if  $2\alpha > 146^\circ$  (although under certain artificial conditions far

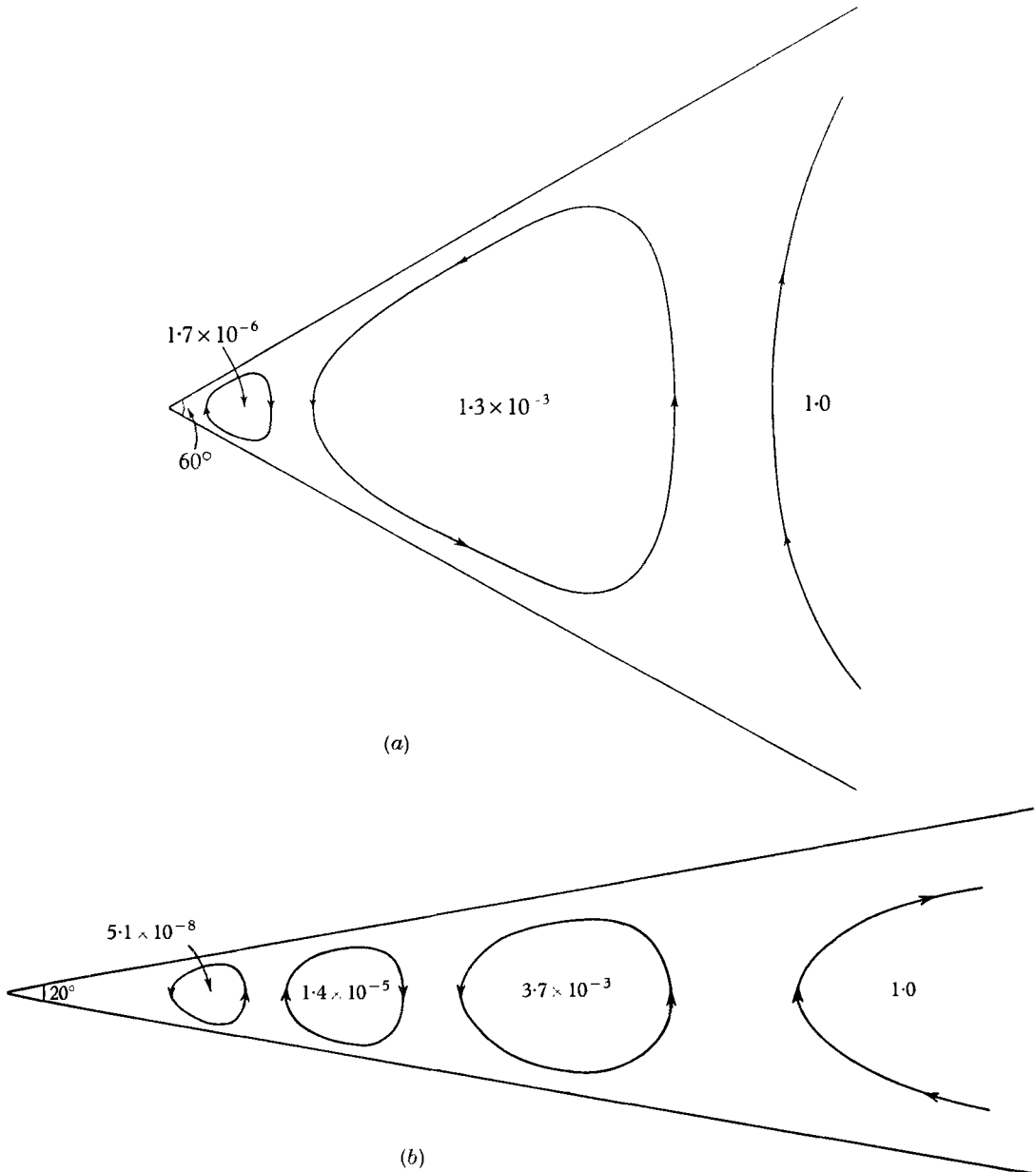


FIGURE 6. Sketch of streamlines in corner eddies (a) for  $2\alpha = 60^\circ$ , (b) for  $2\alpha = 20^\circ$ ; the relative dimensions of these eddies are approximately correct, and the relative intensities are as indicated.

from the corner, the leading coefficients in the expansion (3.1) might vanish, and the critical angle at which eddies disappear would then be greater than  $146^\circ$ .

It is easy, in principle, to derive the equations of the dividing streamlines on which  $\psi = 0$ . For, returning to (3.9), it is clear that  $\psi$  may be written in the form

$$\psi = \left(\frac{r}{r_0}\right)^{p+1} \left\{ \cos\left(q \ln \frac{r}{r_0}\right) \operatorname{Re} g(\theta) - \sin\left(q \ln \frac{r}{r_0}\right) \operatorname{Im} g(\theta) \right\}$$

where  $g(\theta) = A\{\cos \lambda \theta \cos(\lambda - 2)\alpha - \cos(\lambda - 2)\theta \cos \lambda \alpha\}$ .

Hence the dividing streamlines are given by

$$\tan \left[ \frac{\pi}{2} + q \ln \frac{r}{r_0} \right] = \tan \arg g(\theta) = \tan \phi(\theta), \quad \text{say,}$$

so that  $q \ln \frac{r}{r_0} = \phi(\theta) - \frac{\pi}{2} - n\pi \quad (n = 0, 1, 2, \dots)$ ,

or  $r = r_0 \exp \left\{ \frac{1}{q} \left[ \phi(\theta) - \frac{\pi}{2} + n\pi \right] \right\}$ . (3.13)

Since  $\phi(\theta)$  can, in principle, be computed, this equation gives explicitly the shape of the  $n$ th dividing streamline.

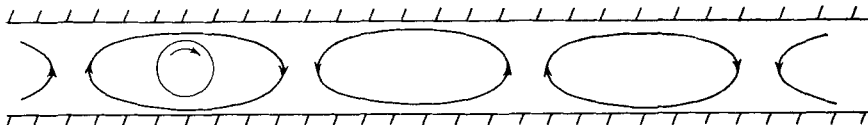


FIGURE 7. The eddy pattern in the limit  $2\alpha \rightarrow 0$ ; the source of the fluid motion is a rotating cylinder between the planes  $y = \pm a$ .

The limiting case  $2\alpha \rightarrow 0$  is of peculiar interest. The limiting form of the stream function  $\psi$  was given (in terms of the complex variable  $z = re^{i\theta}$ ) by Dean & Montagnon, but the implication of a sequence of viscous eddies again seems to have escaped attention. The limit is taken by first fixing one point on each plane (not the vertex) and then allowing the angle  $2\alpha$  to decrease, so that in the limit we consider the flow between two parallel planes at some distance from an arbitrary disturbance. The simplest experimental set-up might be to set the fluid in motion by rotating a cylinder with constant angular velocity between the two planes (figure 7). The appropriate stream function  $\psi$  for the flow at a large distance may be determined either by taking the appropriate limiting form of (3.9), or more simply by looking for a suitable solution of the equation  $\nabla^4 \psi = 0$  of the form

$$\psi \sim f(y) e^{-k|x|}, \quad (3.14)$$

in Cartesian co-ordinates  $(x, y)$ , the origin being in the neighbourhood of the disturbance. If the even function  $f(y)$  satisfying the differential equation, viz.

$$f(y) = A \cos ky + B y \sin ky, \quad (3.15)$$

is made to satisfy the boundary conditions  $f = f' = 0$  on  $y = \pm a$ , the parameter  $k$  is found to satisfy the equation

$$2ka + \sin 2ka = 0,$$

which is simply the limiting form of (3.5) as  $\alpha \rightarrow 0, \mu\alpha \rightarrow ka$ . As already observed, this equation has no real solution, and the relevant imaginary solution (i.e. that with smallest positive real part) is

$$2ka = \lim_{2\alpha \rightarrow 0} (\xi_1 + i\eta_1) \doteq 4 \cdot 21 + 2 \cdot 26i, \quad (3.16)$$

from table 1. The eddies implied by this solution are all of the same size; the wavelength of the disturbance far from the cylinder is approximately

$$\frac{2\pi}{\text{Im } k} = \frac{2\pi \cdot 2a}{2 \cdot 26} = 5 \cdot 56a, \quad (3.17)$$

and the damping factor (i.e. the relative intensity of successive eddies) is approximately

$$\varpi_{\alpha=0} = e^{5 \cdot 87} \approx 350. \quad (3.18)$$

The streamlines must have the form indicated in figure 7.

### 3.2. Flow between a rigid boundary and a free surface

For this type of flow  $f_\lambda(\theta)$  is odd, so that  $A = C = 0$  in (1.2) and

$$f_\lambda(\theta) = B \sin \lambda\theta + D \sin (\lambda - 2)\theta. \quad (3.19)$$

This represents either symmetrical flow between the planes  $\theta = \pm\alpha$  or flow between the rigid boundary  $\theta = -\alpha$  and the free surface  $\theta = 0$ . The boundary conditions in this case lead to the equation

$$\sin 2\mu\alpha = +\mu \sin 2\alpha \quad \text{where} \quad \mu = \lambda - 1. \quad (3.20)$$

This equation has no real solutions if  $\alpha < \alpha_2 \approx 78^\circ$ , and eddies therefore form in the corner between a free surface and a rigid boundary if the angle is less than this critical value.

The imaginary roots  $2\alpha\mu = \xi_2 + i\eta_2$  of (3.20) having the least possible positive value of  $\xi_2$  (between  $2\pi$  and  $\frac{5}{2}\pi$ ) have been calculated and are also listed in table 1. The logarithms of the scale and intensity factors  $\rho_2$  and  $\varpi_2$  which characterize these eddies are also listed. It will be noticed that  $\rho_2 < \rho_1$  for all  $\alpha$ , so that their dimensions fall off less rapidly than those of the corresponding eddies in the former case, but  $\varpi_2 > \varpi_1$  and the intensity in fact falls off very much more rapidly for the second type of eddy.

When  $2\alpha > 2\alpha_2 \approx 156^\circ$ , equation (3.20) has a real root  $\mu$  which decreases from 2.84 when  $2\alpha = 2\alpha_2$  through 2.00 when  $2\alpha = 180^\circ$  to 0.50 when  $2\alpha = 360^\circ$ . This last value gives a stream function proportional to  $r^{\frac{3}{2}}$  representing a symmetrical flow near the leading edge of a flat plate; it is the same as that proposed by Carrier & Lin (1948), for the flow near the leading edge of a flat plate in a uniform stream parallel to the plate.

The stream function again tends to a simple limiting form when  $\alpha \rightarrow 0$ , and describes the flow far from a two-dimensional disturbance in a fluid lying on the plane  $y = 0$  and having a free surface  $y = a$ . The flow once again exhibits eddies, whose dimension in this case is approximately

$$\frac{\pi}{\text{Im } k} = \lim_{\alpha \rightarrow 0} \frac{\pi 2a}{\eta_2} = \frac{2a\pi}{2 \cdot 76} = 2 \cdot 28a$$

in the  $x$ -direction. The damping factor is  $e^{8 \cdot 53} \approx 5000$ , so that to observe even one eddy in this case might be a matter of considerable experimental difficulty.

3.3. *Flow between two free surfaces*

The case of flow between two intersecting free surfaces is perhaps less realistic, although such a situation has been observed in experiments in which a bubble of air rises through a very viscous liquid (B. G. Cox, private communication). It seems worth while including the case here simply by way of contrast with the preceding cases, because it appears that eddies can in no circumstances form near a corner bounded by two free surfaces. The presence of at least one solid boundary is crucial as far as the possible formation of eddies is concerned.

Only the antisymmetric flow between the boundaries  $\theta = \pm \alpha$  is considered, (the symmetrical flow is very similar) and the stream function is again assumed to be of the form (1.1) with

$$f_\lambda(\theta) = A \cos \lambda \theta + B \cos (\lambda - 2) \theta. \quad (3.21)$$

It is assumed that the positions of the free surfaces  $\theta = \pm \alpha$  are maintained by the application of the appropriate pressure distribution which can be calculated from the stream function (3.28). The conditions satisfied on the free surfaces are

$$f_\lambda(\pm \alpha) = f_\lambda''(\pm \alpha) = 0, \quad (3.22)$$

so that

$$A \cos \lambda \alpha + B \cos (\lambda - 2) \alpha = 0, \quad (3.23)$$

and

$$A \lambda^2 \cos \lambda \alpha + B (\lambda - 2)^2 \cos (\lambda - 2) \alpha = 0. \quad (3.23)$$

Hence, eliminating  $A$  and  $B$ ,

$$(\lambda - 1) \cos \lambda \alpha \cos (\lambda - 2) \alpha = 0. \quad (3.24)$$

Now  $\lambda \neq 1$ , for in this case the form (3.21) is inappropriate, so that either

$$\lambda \alpha = (n + \frac{1}{2}) \pi \quad \text{and} \quad B = 0, \quad (3.25)$$

or

$$(\lambda - 2) \alpha = (n + \frac{1}{2}) \pi \quad \text{and} \quad A = 0, \quad (3.26)$$

where  $n$  is any integer. Thus  $\lambda$  is real, precluding the possibility of eddies; and choosing the smallest possible value of  $\lambda$  not less than unity gives

$$\lambda = \begin{cases} 2 - \pi/2\alpha & \text{if } 2\alpha > \pi \\ \pi/2\alpha & \text{if } 2\alpha \leq \pi \end{cases} \quad (3.27)$$

with corresponding stream functions

$$\psi = \begin{cases} Br^{2-\pi/2\alpha} \cos(\pi\theta/2\alpha) & \text{if } 2\alpha > \pi, \\ Ar^{\pi/2\alpha} \cos(\pi\theta/2\alpha) & \text{if } 2\alpha \leq \pi. \end{cases} \quad (3.28)$$

The flow sufficiently near the corner is therefore rotational if  $2\alpha > \pi$ , but irrotational if  $2\alpha \leq \pi$ . These results are in striking contrast with those obtained in §§ 3.1 and 3.2.

The situation here contemplated is artificial to the extent that an appropriate pressure distribution must be applied on the planes  $\theta = \pm \alpha$  in order to balance the total normal stress implied by the stream-function (3.28). In the context of the bubble problem, it is relevant to inquire whether this pressure can be pro-

vided by the motion (possibly rotational) of a nearly inviscid fluid in the region  $|\theta| > \alpha$ ; but this problem is rather far removed from the central topic of this paper and will not be pursued further here.

#### 4. The asymptotic flow at a large distance induced by a disturbance near the corner

All the results obtained in §3 may be reinterpreted in terms of the flow at a large distance from a corner induced by a disturbance near the corner (e.g. a line source of vorticity at the corner). It was observed in the introduction that the Stokes approximation is valid far from the corner if the real part of the exponent  $\lambda$  of the stream function describing the flow is negative. It is therefore natural to look again for a stream function of the form (1.1) with  $\text{Re}(\lambda) < 0$  satisfying a set of four boundary conditions corresponding to either rigid or free boundaries.

The same relations for the exponent (equations (3.5) and (3.20)) are obtained in the cases considered in §§3.1 and 3.2. Clearly if either of these equations is satisfied by  $\mu (= \lambda - 1) = \mu_1$ , say, then it is also satisfied by  $\mu = -\mu_1$ . This provides the interesting result that if  $\psi = r^\lambda f_\lambda(\theta)$  ( $\text{Re}(\lambda) > 1$ ) is the Stokes flow *near* a corner between either two rigid boundaries (case (i)) or a rigid boundary and a free surface (case (ii)), then

$$\psi = r^{-\lambda+2} f_{-\lambda+2}(\theta) \quad (4.1)$$

is a solution of the Stokes equation  $\nabla^4 \psi$  representing a flow *far* from a corner of the same angle, and satisfying the correct boundary conditions (in either case); the velocity components of the corresponding flow fall off as  $r^{-\lambda+1}$  for large  $r$ . Only if  $\text{Re}(\lambda) > 2$  does the corresponding Reynolds number decrease as  $r$  increases. This condition is satisfied provided

$$\left. \begin{aligned} 2\alpha < 180^\circ & \text{ in case (i),} \\ \alpha \lesssim 126^\circ & \text{ in case (ii),} \end{aligned} \right\} \quad (4.2)$$

so that, in particular, in all cases where eddies exist, the form (4.1) provides an asymptotic flow consistent with the Stokes approximation. The dimensions and intensities of adjacent eddies are again in the same ratios (for a given angle) as before, but the intensities now decrease with increasing distance from the corner. The flow patterns of figure 6 may now be reinterpreted as the flow induced far from the corner by a general disturbance near the corner, but with the indicated intensities in reverse order.

If  $\alpha$  exceeds either of the limits set by (4.2) the velocities implied by the stream function (4.1) fall off more slowly than  $r^{-1}$ , and at a large distance from the corner inertia forces must be taken into account, even if velocities near the corner are small enough for the Stokes approximation to be valid.

Similar observations may be made regarding the flow between two free surfaces, but the case is too artificial to merit further consideration here.

#### 5. The effect of an electric current along the intersection of the two planes

Returning now to the problem of flow near a sharp corner, we suppose that the fluid is endowed with electrical conductivity  $\sigma$  and magnetic permeability  $\mu$ ,

and we investigate the effect of a line current  $J$  along the intersection of the two planes. It is intended only to demonstrate the qualitative effect of such a current, and only one case will be considered, viz. that of antisymmetric flow between two rigid boundaries  $\theta = \pm \alpha$ . The magnetic Reynolds number  $R_m$ , based on the velocity at distance  $r$  from 0, is proportional to the Reynolds number  $R$

$$R_m(r) = 4\pi\mu\sigma\nu R(r) \quad (\text{Gaussian units}). \quad (5.1)$$

Hence, sufficiently near 0,  $R_m$  as well as  $R$  will be small. In fact, for typical laboratory materials,  $4\pi\mu\sigma\nu \ll 1$ , so that the approximation  $R_m \ll 1$  is likely to be valid over a much wider range than the approximation  $R \ll 1$ .

The magnetic field due to the current  $J$  is

$$\mathbf{H}_0 = \left(0, \frac{2J}{r}, 0\right), \quad (5.2)$$

and the induced current in the fluid is

$$\mathbf{j} = \sigma\mathbf{u} \wedge \mathbf{H}_0 = \left(0, 0, \frac{2\sigma J u}{r}\right), \quad (5.3)$$

(in the assumed absence of any applied electric field in the  $z$ -direction). The Lorentz body force in the fluid is then

$$\mu\mathbf{j} \wedge \mathbf{H}_0 = \left(-\frac{4M^2\nu u}{r^2}, 0, 0\right), \quad (5.4)$$

where

$$M = \mu\sigma^{\frac{1}{2}}J/\nu^{\frac{1}{2}}. \quad (5.5)$$

$M$  is the appropriate Hartmann number for the problem. This body force is a radial force opposing the radial velocity and may therefore be expected to promote the formation of eddies near the corner.

The linearized vorticity equation becomes

$$4M^2 \nabla \wedge \left(\frac{u}{r^2}, 0, 0\right) = \nabla^2 \boldsymbol{\omega},$$

or, with the substitution

$$\begin{aligned} u &= \frac{1}{r} \frac{\partial \psi}{\partial \theta}, \quad \boldsymbol{\omega} = -\nabla^2 \psi \mathbf{k}, \\ \nabla^4 \psi &= \frac{4M^2}{r^4} \frac{\partial^2 \psi}{\partial \theta^2}. \end{aligned} \quad (5.6)$$

If  $\psi \propto r^\lambda f_\lambda(\theta)$ , the equation for  $f_\lambda(\theta)$  becomes

$$\left[(\lambda - 2)^2 + \frac{d^2}{d\theta^2}\right] \left[\lambda^2 + \frac{d^2}{d\theta^2}\right] f_\lambda - 4M^2 f_\lambda'' = 0. \quad (5.7)$$

For general  $M$ , the problem of determining  $\lambda$  is straightforward, though tedious; the general even solution of (5.7) is of the form

$$f_\lambda = A \cos p_1 \theta + C \cos p_2 \theta, \quad (5.8)$$

where  $p_1^2(\lambda)$  and  $p_2^2(\lambda)$  are the roots of the quadratic equation associated with (5.7). The function (5.8) satisfies  $f_\lambda(\pm \alpha) = f_\lambda'(\pm \alpha) = 0$  provided

$$p_1 \tan p_1 \alpha = p_2 \tan p_2 \alpha, \quad (5.9)$$



an equation that defines implicitly the possible values of  $\lambda$ . Clearly these values could be found numerically.

There is one case, however, which can be analysed without recourse to numerical methods, and which sufficiently indicates the trend. This is the case  $M = 1$ , when (5.7) may be reduced to the simpler form

$$[d^2/d\theta^2 + \lambda(\lambda - 2)]^2 f_\lambda = 0, \quad (5.10)$$

with general even solution

$$f_\lambda = A \cos \mu\theta + D\theta \sin \mu\theta, \quad (5.11)$$

where

$$\mu = +[\lambda(\lambda - 2)]^{\frac{1}{2}}, \quad (5.12)$$

(the root with positive real part being chosen). The boundary conditions  $f_\lambda = f'_\lambda = 0$  on  $\theta = \pm\alpha$  imply that

$$\begin{aligned} A \cos \mu\alpha + D\alpha \sin \mu\alpha &= 0, \\ -A\mu \sin \mu\alpha + D \sin \mu\alpha + D\mu\alpha \cos \mu\alpha &= 0, \end{aligned}$$

so that, eliminating the ratio  $A/D$ ,

$$\sin 2\mu\alpha + 2\mu\alpha = 0. \quad (5.13)$$

This equation admits no real solutions (other than the irrelevant one  $\mu = 0$ ) no matter what the angle  $\alpha$ . It does, however, admit complex solutions, the one with least positive real part being

$$\mu = \mu_1 = (2\alpha)^{-1}(\xi_0 + i\eta_0), \quad (5.14)$$

where  $\xi_0 \doteq 4.21$ ,  $\eta_0 \doteq 2.26$  are simply the roots of (3.6) with  $k = 1$ . The corresponding value of  $\lambda$ , from (5.12), is

$$\begin{aligned} \lambda &= 1 \pm (1 + \mu^2)^{\frac{1}{2}} \\ &= 1 \pm (2\alpha)^{-1} [4\alpha^2 + \xi_0^2 - \eta_0^2 + 2i\xi_0 \eta_0]^{\frac{1}{2}} \\ &\doteq 1 + (2\alpha)^{-1} (4\alpha^2 + 12.2 + 19.2i)^{\frac{1}{2}}, \end{aligned}$$

(the positive sign being chosen to make  $\text{Re}(\lambda) > 1$ ). This value of  $\lambda$  has been calculated for a few different values of  $2\alpha$ , and it is compared in table 2 with the corresponding value of  $\lambda$  in the absence of a magnetic field. The most striking effect of the magnetic field is that reversed flow and eddies now form for any angle  $2\alpha$  (including reflex angles). The eddies that form in such a case are the direct result of the increased ohmic dissipation of energy, and they may fairly be called resistive in type. It is reasonable now to infer that as  $M$  increases from 0 to some value  $M_c \leq 1$ , the maximum corner angle for which eddies form increases from  $146^\circ$  to  $360^\circ$  (there is no reason to suspect non-uniform behaviour in the limit  $M \rightarrow 0$ ); and that for  $M > M_c$ , corner eddies invariably form for *any* angle  $2\alpha$ .

The other effect of the magnetic field, indicated by the results of table 2, is that the real part of  $\lambda$  is greater when  $M = 1$  than when  $M = 0$ , an effect that is very slight for small angles, but pronounced for reflex angles. This means that the velocity falls off more rapidly as the corner is approached when electric currents are present, as might be expected in view of the second available sink of energy in this region.

The imaginary part of  $\lambda$  is small for reflex angles in the case  $M = 1$ , so that the ratio of the dimensions of consecutive eddies is also small. It seems likely, however, that as  $M$  increases the tendency for  $\text{Im}(\lambda)$  to increase (for any angle) will

$2\alpha^\circ$	$\lambda$ $M = 1$	$\lambda$ $M = 0$
20	$13 + 6.3i$	$13 + 6.2i$
90	$3.8 + 1.4i$	$3.8 + 1.1i$
140	$2.9 + 0.82i$	$2.8 + 0.25i$
360	$2.1 + 0.021i$	1.5

TABLE 2. The effect of the electric current on the exponent  $\lambda$ .

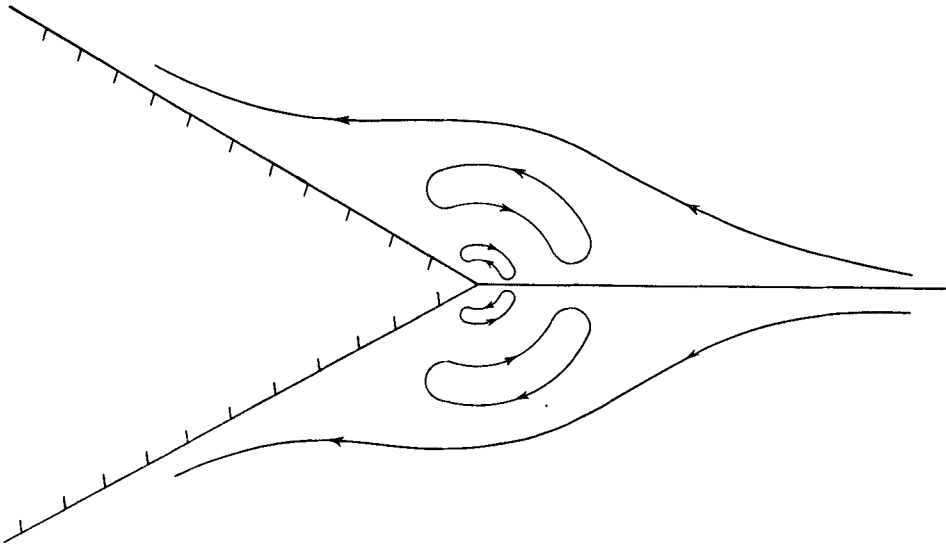


FIGURE 8. Sketch of the symmetric eddy pattern in the flow past a wedge vertex at high Hartmann number. An electric current  $J$  flows along the intersection of the two planes.

continue, and that the ratio of dimensions of consecutive eddies will correspondingly increase. The type of streamline pattern suggested by these considerations for the symmetric flow at large  $M$  near a wedge vertex is sketched in figure 8.

#### REFERENCES

- CARRIER, G. F. & LIN, C. C. 1948 *Quart. Appl. Math.* **6**, 63.  
 DEAN, W. R. & MONTAGNON, P. E. 1949 *Proc. Camb. Phil. Soc.* **45**, 389.  
 JEFFERY, G. B. 1915 *Phil. Mag.* **29**, 455.  
 MOFFATT, H. K. 1964 *Arch. Mech. Stosowanej* (in the Press).  
 RAYLEIGH, LORD 1920 *Sci. Pap.* **6**, 18.  
 TAYLOR, G. I. 1960 *Aeronautics and Astronautics*, p. 12, ed. Hoff & Vincenti, Pergamon Press.